Multilag Frequency Estimation for High-Order BOC Signals in the Acquisition Stage

David Gómez-Casco*, Elena Simona Lohan†, José A. López-Salcedo* and Gonzalo Seco-Granados*
*Department of Telecommunications and Systems Engineering,
Universitat Autònoma de Barcelona (UAB), Bellaterra, Spain
† Institute of Communications Engineering, Tampere University of Technology, Finland

***Abstract*—In the context of global navigation satellite systems, this paper addresses the problem of refining the Doppler frequency estimation provided in the acquisition stage for high-order binary offset carrier (BOC) signals in post-correlation. The refinement of Doppler frequency must be done because the estimation obtained from the acquisition stage is not usually accurate enough to track the signal in the tracking stage. In this work, we only use the cross-ambiguity function (CAF) created in the acquisition stage to perform the refinement. A least squares estimator has been already applied to mitigate this problem. We propose a new technique, referred to as multilag least squares estimator, which improves the performance of the least squares estimator by exploiting the autocorrelation shape of high-order BOC signals. Moreover, the Cramer-Rao bound and the expected Cramer-Rao bound are derived as benchmark to compare the performance of the least squares and multilag least squares estimators.**

I. Introduction

The main task of the acquisition stage of a global navigation satellite systems (GNSS) receiver is to obtain a coarse estimation of the code-delay and the Doppler frequency for each satellite in view. After that, these estimations are tracked and refined to accurately follow any possible variation of time and frequency at the tracking stage [1]. Nevertheless, many times the coarse estimation of Doppler frequency provided by the acquisition stage is not accurate enough to pass directly to the tracking stage. In that situation, the accuracy of the Doppler frequency estimation must be improved before starting the tracking stage. This process is usually carried out in GNSS by a frequency lock loop (FLL) [2], [3]. However, the downside of the FLL is that it needs a particular architecture and some additional data [4].

Another alternative is introduced in [5]. This method refines the coarse Doppler frequency estimation obtained in the acquisition stage by applying an interpolation method, but the fundamental of this method is based on an empirical approximation. Another approach is used [4]. This method estimates the Doppler frequency by application of a formula, but it only works properly when the receiver uses a specific configuration to acquire the signal.

An additional technique is proposed in [6]. The proposed technique estimates the Doppler frequency by performing a least squares (LS) estimator in post-correlation. Moreover, this method can be implemented in any receiver because it depends only on the cross-ambiguity function (CAF) computed in the acquisition stage. This technique has been used with a Galileo E1BC signal [7], which is a low-order binary offset carrier (BOC) signal, obtaining an accurate estimation of the Doppler frequency. In this work, we focus on estimating the Doppler frequency of high-order BOC signals, which are being implemented by new generations of GNSS.

The high-order BOC modulations provide greater accuracy than conventional BPSK and low-order BOC modulations in terms of positioning since the main peak of a high-order BOC correlation is narrower. The drawback of the BOC modulations is that their correlation functions become ambiguous because they are formed by several peaks. The larger the order of the BOC signal, the larger the number of secondary peaks. The existence of secondary peaks is usually a dramatic problem since they do not allow us to identify the main peak of the correlation function, especially in high-order BOC signals [8], [9], [10], [11], [12]. Nonetheless, the characteristic multi-peaked of high-order BOC correlations can lead to a more accurate estimation of the Doppler frequency in post-correlation. This is because the secondary peaks of high-order BOC correlations contain a lot of energy and it can be used to improve the Doppler frequency estimation provided by the acquisition stage.

In this paper, we propose a new technique, referred to as multilag least squares estimator (MLS), to refine the coarse Doppler frequency estimation provided by the acquisition stage, especially for high-order BOC signals, which outperforms the estimator proposed in [6]. The MLS estimator can be implemented in any GNSS receiver since it is applied in the acquisition stage and it does not depend on any parameter of the receiver. The proposed technique herein exploits the characteristic multi-peaked of these signals to increase the precision of the Doppler frequency estimation. In addition to this, the Cramer-Rao bound (CRB) and the expected CRB of the Doppler frequency estimation are derived as benchmark to compare the performance of the LS and MLS estimators.

II. Signal Model

The baseband form of a received GNSS signal can be represented as follows [13]:

$$r[n] = \sum_{t=1}^{P} \tilde{A}_t b_t(nT_s-\tau_t)s_t(nT_s-\tau_t)c_t(nT_s-\tau_t) \times e^{j(2\pi f_{d,t} nT_s+\tilde{\theta}_t)} + \tilde{\omega}[n], \quad (1)$$

978-1-5090-3885-5/16/$31.00 ©2016 IEEE

where P is the satellites number, T_s is the sampling interval, $\tilde{A}_t$ is the received amplitude of the tth satellite, $b_t(nT_s-\tau_t)$ is the unknown navigation data bit, $s_t(nT_s-\tau_t)$ is the subcarrier used to modulate the signal like a high-order BOC (when $s_t(nT_s-\tau_t)=1$ the subcarrier does not exist and then the signal is modulated as a conventional BPSK), $c_t(nT_s-\tau_t)$ is the pseudo random noise code, τ_t is the code-delay from the tth satellite to the receiver, $\tilde{\theta}_t$ is the carrier phase of the received signal, $f_{d,t}$ is the Doppler frequency owing to the movement of the satellite, and $\tilde{\omega}[n]$ is the complex additive white Gaussian noise (AWGN).

The first task that a GNSS receiver must perform is to acquire the signals from the satellites currently in view. To do so, the received signal $r[n]$ is correlated by the different local replicas of the transmitted signals from the P satellites with tentative values of code-delay and Doppler frequency. Nonetheless, in this paper, we focus on acquiring only one satellite, for instance the kth satellite, because it is enough to analyze the performance of the frequency estimation. The local replica of the kth satellite using different tentative values of the code-delay τ_k and the Doppler frequency $f_{d,k}$ as $\tilde{\tau}_k$ and $\tilde{f}_{d,k}$, respectively, is given by

$$x[n]=s_k(nT_s-\tilde{\tau}_k)c_k(nT_s-\tilde{\tau}_k)e^{j(2\pi\tilde{f}_{d,k}nT_s)}. \quad (2)$$

The tentative values $\tilde{\tau}_k$ and $\tilde{f}_{d,k}$ span all the possible values of $f_{d,k}$ and τ_k doing a bidimensional search to find the correlation peak. The correlation between $r[n]$ and $x[n]$ is so-called the output of the coherent integration or CAF [14] and it can be written, in absence of navigation data bit, as

$$\begin{aligned} R(\tilde{\tau}_k,\tilde{f}_{d,k}) &= \sum_{n=1}^{L_{ch}} r[n]s_k(nT_s-\tilde{\tau}_k)c_k(nT_s-\tilde{\tau}_k)e^{j(2\pi\tilde{f}_{d,k}nT_s)} \\ &= A_k e^{j\theta_k}\mathrm{sinc}(\Delta f T_{coh})v(\Delta\tau)+\omega_k, \end{aligned} \quad (3)$$

where A_k is the complex received amplitude with phase θ_k of the kth satellite after computing the CAF, $\Delta f=f_{d,k}-\tilde{f}_{d,k}$ is the residual frequency offset, $\Delta\tau=\tau_k-\tilde{\tau}_k$ is the residual delay offset between the received GNSS signal and the local replica, $v(\Delta\tau)$ is the autocorrelation function of a GNSS signal, T_{coh} is the coherent integration time, L_{ch} is the samples number integrated coherently and ω_k is AWGN after performing the coherent integration with zero-mean and variance σ^2. The coherent integration losses due to the residual frequency error are given by the $\mathrm{sinc}(\Delta f T_{coh})$ term.

The ideal CAF in time domain of a BPSK modulation is unambiguous because it only exhibits one peak (without taking into account Doppler effects nor noise). However, the ideal CAF in time domain of a $\mathrm{BOC_{cos}}(15,2.5)$ modulation, as a representative case of high-order BOC signals, is ambiguous because it shows several peaks. More precisely, the $\mathrm{BOC_{cos}}(15,2.5)$ correlation contains 25 peaks taking into account the positive and negative peaks. This fact is because the total number of peaks of a $\mathrm{BOC_{cos}}$ correlation is $2K_{BOC}+1$, where $K_{BOC}=\frac{2f_{sub}}{f_c}$ with $f_{sub}=15\cdot 1.023$ MHz and $f_c=2.5\cdot 1.023$ MHz. The high-order BOC modulations provide an estimation of the code-delay more accurate than

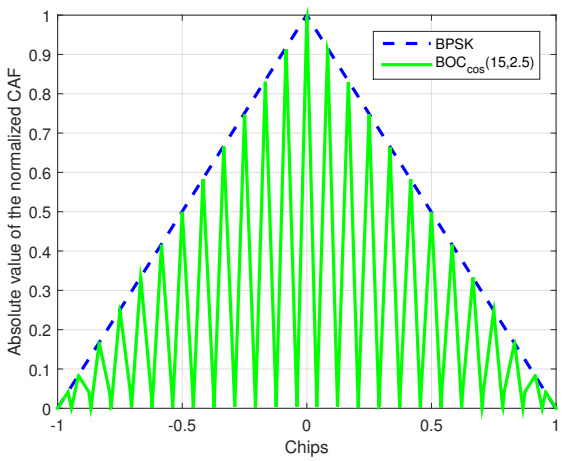

Fig. 1. Comparison between the CAF in time domain of the BPSK and $\mathrm{BOC_{cos}}(15,2.5)$ signals.

BPSK modulation with the disadvantage of becoming its CAF in ambiguous owing to the apparition of secondary peaks. The comparison between the absolute value of the CAF in time domain of the BPSK and $\mathrm{BOC_{cos}}(15,2.5)$ signals is shown in Fig 1. In any case, the process to acquire the satellite is always the same: calculating the CAF independently of the modulation used. After performing the CAF, its absolute value is computed as

$$Z(\tilde{\tau}_k,\tilde{f}_{d,k})=|R(\tilde{\tau}_k,\tilde{f}_{d,k})|. \quad (4)$$

In order to detect if the satellite is in view or the satellite is not in view, the maximum magnitude of (4) is compared with a signal detection threshold. The satellite is not in view if the maximum magnitude of (4) does not exceed the detection threshold. Nevertheless, if the maximum magnitude of (4) exceeds the signal detection threshold the satellite is considered in view and a coarse estimation of the τ_k and $f_{d,k}$ is obtained as $\hat{\tau}_k$ and $\hat{f}_{d,k}$.

In acquisition stage, the accuracy of the $\hat{\tau}_k$ is usually given by the sampling frequency, denoted as f_s, used at the receiver. The error of $\hat{f}_{d,k}$ is comprised between the range $[-f_{st}/2, f_{st}/2]$, where f_{st} is the search step of Doppler frequency used in the local replica to compute the CAF. The f_{st} is chosen taking into account a trade-off between the complexity in terms of computational burden at the receiver and the accuracy in the estimation of Doppler frequency. A typical value of f_{st} to mitigate the coherent integration losses is $1/(2T_{coh})$. However, many times the estimation $\hat{f}_{d,k}$ is not precise enough to track the signal in the tracking stage. For this reason, a more accurate estimation of $f_{d,k}$ must be done before starting the tracking stage.

III. Fine Frequency Estimation

According to the estimation theory, the best estimator to estimate $f_{d,k}$ is the maximum likelihood (ML). In this case, the ML is the value that maximizes the magnitude of the CAF

978-1-5090-3885-5/16/$31.00 ©2016 IEEE

in (3). Nonetheless, it is not possible to apply this estimator in practice to find an accurate estimation of $f_{d,k}$ since this estimator has a high computational complexity. Then, we must resort to other alternatives to get a precise estimation of $f_{d,k}$ [4].

One way to obtain a fine Doppler frequency estimation is by the use of a FLL. However, the FLLs need a particular architecture using filters, numerical control oscillators and some additional data. Moreover, the FLLs are usually integrated inside the tracking loop and more and more GNSS receivers are using an open-loop architecture, which do not have a tracking loop. Another alternative was proposed in [6], which improves the Doppler frequency estimation based only on the CAF obtained from the acquisition stage by using a LS estimator in post-correlation.

A. Least squares estimator

As we have already mentioned, the degradation produced in the CAF by the residual Doppler frequency between the received signal and the local replica is affected by a sinc function. This method exploits this fact to refine the coarse Doppler frequency estimation obtained in the acquisition stage [6]. More precisely, the method consists in finding the Doppler frequency value that provides the best fit between the theoretical sinc function and the measured one. To do so, let us define the received or the measured sinc function in a vector $\mathbf{g}$ containing a set of 3 samples: the maximum value of the CAF in (4) and the two adjacent values of the CAF in the frequency domain for the estimation of $\hat{\tau}_k$ as

$$\mathbf{g} = \begin{bmatrix} Z(\hat{\tau}_k, \hat{f}_{d,k} - f_{st}) \\ Z(\hat{\tau}_k, \hat{f}_{d,k}) \\ Z(\hat{\tau}_k, \hat{f}_{d,k} + f_{st}) \end{bmatrix}. \quad (5)$$

We define the vector $\mathbf{t}(f_{d,k})$ containing also 3 samples of the theoretical sinc function with an unknown Doppler frequency:

$$\mathbf{t}(f_{d,k}) = \begin{bmatrix} |\mathrm{sinc}((f_{d,k} - f_{st})T_{coh})| \\ |\mathrm{sinc}((f_{d,k})T_{coh})| \\ |\mathrm{sinc}((f_{d,k} + f_{st})T_{coh})| \end{bmatrix}. \quad (6)$$

It should be added that we only take three points to define the vectors $\mathbf{g}$ and $\mathbf{t}(f_{d,k})$ because we want to guarantee that the three chosen points are located in the main lobe of the sinc function. We do not take more points of the sinc function since the rest of the points contain almost no signal and in presence of noise, they may cause a worsening of the fine Doppler estimation of $f_{d,k}$. Fig. 2 shows an illustrative plot of the expected theoretical sinc function, the measured sinc function obtained from the acquisition stage, and the Doppler frequency of the received signal.

The fine Doppler frequency estimation of $f_{d,k}$ is carried out by minimizing the following non-linear LS cost function:

$$J(\beta, f_{d,k}) = ||\mathbf{g} - \beta\mathbf{t}(f_{d,k})||^2, \quad (7)$$

where β is the unknown amplitude due to the propagation effects of the received signal. The non-linear LS, which is affected by two unknown parameters $f_{d,k}$ and β, can be minimized by separation of variables in two steps [15]. Firstly, the non-linear LS is minimized with respect to β so that the cost function depends only on $f_{d,k}$. The unknown amplitude that minimize the function J is $\hat{\beta} = (\mathbf{t}(f_{d,k})^T\mathbf{t}(f_{d,k}))^{-1}\mathbf{t}(f_{d,k})^T\mathbf{g}$. Replacing this expression in (7), we get

$$J(\hat{\beta}, f_{d,k}) = ||\mathbf{g} - (\mathbf{t}(f_{d,k})^T\mathbf{t}(f_{d,k}))^{-1}\mathbf{t}(f_{d,k})^T\mathbf{g}\mathbf{t}(f_{d,k})||^2. \quad (8)$$

Secondly, the problem now reduces to minimize (8). The cost function must be minimized by the application of an iterative algorithm since there is no analytical solution in a closed-form for $f_{d,k}$. In our simulation, we use simple for loop to estimate the value of $f_{d,k}$.

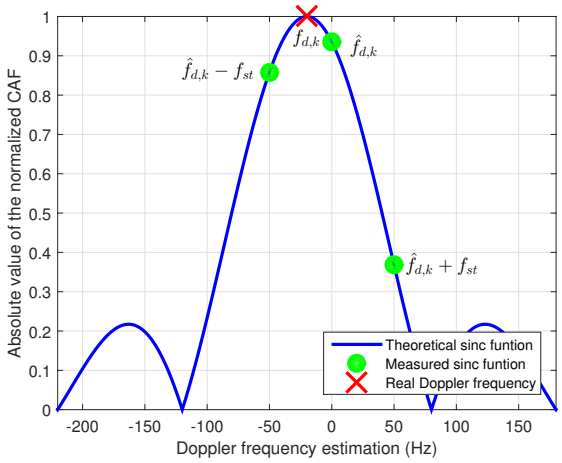

Fig. 2. Illustrative plot of the CAF in frequency domain.

B. Multilag least squares estimator

In this subsection, we propose a novel contribution for estimating the $f_{d,k}$ in the acquisition stage referred to herein as multilag least squares (MLS) estimator, especially for high-order BOC signals. We want to exploit that the ideal CAF in time domain of a high-order BOC signal contains a considerable number of secondary peaks. Moreover, the received signal is always impacted by the sampling frequency used and this causes that many times the high-order BOC signals are not sampled in the maximum of the CAF since the signal arrives with an unknown random code-delay. One example of the ideal CAF of a $\mathrm{BOC}_{\cos}(15,2.5)$ signal in time domain and the received CAF using a $f_s = 50$ MHz, which is the maximum value of a USRP nowadays [16], is shown in Fig. 3. The received CAF often exhibits some high peaks with practically the same magnitude, which may be a useful tool to estimate $f_{d,k}$ of a more effective way in terms of accuracy than the estimator explained in III-A.

The method explained in III-A only uses the maximum value of the CAF and the two adjacent values of the CAF in frequency domain. Nonetheless, we propose to use the different large values of the CAF in time domain (including the maximum value) and each large value with their two adjacent

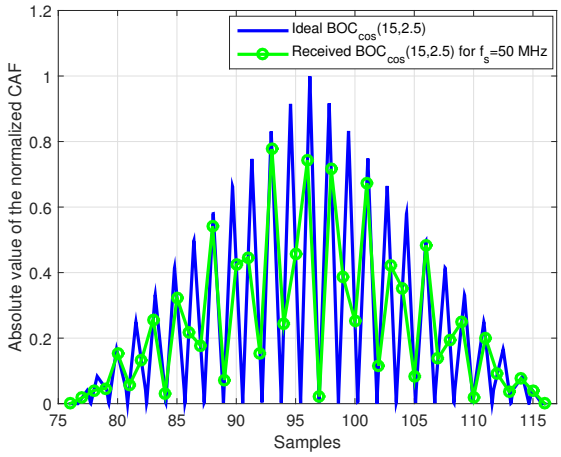

Fig. 3. Illustrative plot of the ideal CAF of a $\text{BOC}_{\cos}(15,2.5)$ signal in time domain and the received CAF using a $f_s = 50$ MHz (without taking into account the noise and the Doppler effect).

values of the CAF in frequency domain. This approach can be solved by minimizing the distance between two matrices. The method proposed herein deals with the estimation of Doppler frequency by finding the best fit between the theoretical sinc functions and the different measured sinc functions. Before proceeding, we denote the magnitude of the second largest value of the CAF in time domain as β_2 with argument τ_k^2 and the magnitude of the thirst largest value of the CAF in time domain as β_3 with argument τ_k^3 and so on. Thereby, let us define the $C \times 3$ matrix $\mathbf{G}$, with C the number of chosen large values of the CAF in time domain, containing the different measured sinc functions from each large value as

$$\mathbf{G} = \begin{bmatrix} Z(\hat{\tau}_k, \hat{f}_{d,k} - f_{st}) & Z(\hat{\tau}_k, \hat{f}_{d,k}) & Z(\hat{\tau}_k, \hat{f}_{d,k} + f_{st}) \\ Z(\hat{\tau}_k^2, \hat{f}_{d,k} - f_{st}) & Z(\hat{\tau}_k^2, \hat{f}_{d,k}) & Z(\hat{\tau}_k^2, \hat{f}_{d,k} + f_{st}) \\ Z(\hat{\tau}_k^3, \hat{f}_{d,k} - f_{st}) & Z(\hat{\tau}_k^3, \hat{f}_{d,k}) & Z(\hat{\tau}_k^3, \hat{f}_{d,k} + f_{st}) \\ \vdots & \vdots & \vdots \\ Z(\hat{\tau}_k^C, \hat{f}_{d,k} - f_{st}) & Z(\hat{\tau}_k^C, \hat{f}_{d,k}) & Z(\hat{\tau}_k^C, \hat{f}_{d,k} + f_{st}) \end{bmatrix}. \quad (9)$$

The cost function can be expressed by the Frobenius distance as

$$H(\mathbf{a}, f_{d,k}) = ||\mathbf{G} - \mathbf{a} \cdot \mathbf{t}(f_{d,k})^T||_F^2, \quad (10)$$

where the vector $\mathbf{a} = [\beta, \beta_2, \beta_3, \cdots, \beta_C]^T$ have all the unknown amplitudes, one unknown amplitude for each chosen large value and $\mathbf{t}(f_{d,k})$ is defined in (6). The estimation of $f_{d,k}$ is the value that minimize the cost function. To minimize this problem, we apply separability of variable because the vector $\mathbf{a}$ is linearly dependent over $\mathbf{t}$. Then, we must replace $\hat{\mathbf{a}} = \frac{\mathbf{G} \cdot \mathbf{t}(f_{d,k})}{||\mathbf{t}(f_{d,k})||^2}$ by $\mathbf{a}$ in (10). Thus,

$$H(\hat{\mathbf{a}}, f_{d,k}) = \left|\left| \mathbf{G} - \frac{\mathbf{G} \cdot \mathbf{t}(f_{d,k})}{||\mathbf{t}(f_{d,k})||^2} \mathbf{t}(f_{d,k})^T \right|\right|_F^2. \quad (11)$$

After that, the fine estimation of $f_{d,k}$ is found by applying an iterative algorithm since there is not any analytical solution in closed-form. In this case, we also use a simple for loop to minimize the cost function.

C. Cramer-Rao bound

Theoretical lower bounds become necessary for evaluating the performance of the proposed estimators in the Subsections III-A and III-B. The CRB, which expresses a lower bound on the variance of any unbiased estimator, provides a benchmark to compare the performance of the LS and MLS estimators. The CRB is defined by:

$$\text{var}(\hat{f}_{d,k}) \geq \text{CRB}(f_{d,k}) = -\left[E\left[\frac{\partial^2}{\partial f_{d,k}^2} \ln p_r(\mathbf{r}; f_{d,k}) \right] \right]^{-1}, \quad (12)$$

where $E[\cdot]$ is the expected operator, $\mathbf{r}$ is a vector containing the L_{ch} samples of the received signal and $p_r(\mathbf{r}; f_{d,k})$ is the probability density function of the received signal. The CRB of the Doppler frequency estimation in an AWGN channel is given by [17]

$$\text{var}(\hat{f}_{d,k}) \geq \frac{6}{(2\pi)^2 \text{SNR} T_s^2 L_{ch}(L_{ch}^2 - 1)}, \quad (13)$$

where $\text{SNR} = A^2/\sigma^2$ and $T_s = 1/f_s$. Assuming that $L_{ch} = f_s T_{coh} >> 1$ the CRB is written as follows:

$$\text{var}(\hat{f}_{d,k}) \geq \frac{6}{(2\pi)^2 \text{SNR} f_s T_{coh}^3}. \quad (14)$$

Typically, the SNR is not a parameter used in GNSS since it depends on the receiver front-end bandwidth denoted as B. The parameter usually utilized to analyze the performance of techniques is the carrier-to-noise ratio (C/N_0), which is not affected by the receiver bandwidth. The relationship between the SNR and the C/N_0 is given by

$$\text{SNR} = \frac{C}{N_0 B}. \quad (15)$$

The CRB in (14) is the bound for the estimation of $f_{d,k}$ because it takes into account the C/N_0 from the received signal. However, often in post-correlation, we do not get a C/N_0 as high as in pre-correlation since the received CAF many times exhibits some high peaks, but none of them match with the real peak of the CAF (Fig. 3). This fact causes a degradation at post-correlation in terms of C/N_0, which is due to the sampling frequency and the unknown random code-delay of the received signal. In order to obtain a benchmark for the received C/N_0 in post-correlation, we must resort to the Expected CRB (ECRB) [18].

D. Expected Cramer-Rao bound

The effect introduced by the unknown random code-delay is measured taking into account the term $\widetilde{\Delta\tau}$ in the SNR expression. The SNR considering the degradation provided by the random code-delay is expressed as

$$\widetilde{\text{SNR}} = \frac{A^2 |\nu(\widetilde{\Delta\tau})|^2}{\sigma^2}, \quad (16)$$

978-1-5090-3885-5/16/$31.00 ©2016 IEEE

where $\widetilde{\Delta\tau} = \tau_k - \hat{\tau}_k$ and $v(\widetilde{\Delta\tau})$ is the normalized autocorrelation function of the GNSS signal with a value equal to 1 for $\widetilde{\Delta\tau} = 0$ and values smaller than 1 for $\widetilde{\Delta\tau} \neq 0$. Then, the $v(\widetilde{\Delta\tau})$ provides an attenuation in the received signal, which increases the value of the CRB computed in III-C. The variable $v(\widetilde{\Delta\tau})$ follows a uniform distribution because the signal can be received with any value of code-delay. To avoid the obstacle of the random variable $v(\widetilde{\Delta\tau})$, we can compute the $\mathrm{ECRB}(f_{d,k}) = E[\mathrm{CRB}(f_{d,k})]$ as

$$-E_{v(\widetilde{\Delta\tau})}\left[\left[E_{\mathbf{r}}\left[\frac{\partial^2}{\partial f_{d,k}^2}\ln p_r(\mathbf{r}; f_{d,k}, v(\widetilde{\Delta\tau}))\right]\right]^{-1}\right]. \quad (17)$$

The resulting ECRB is the same as in (14), but applying the expectation operation as

$$\mathrm{ECRB}(f_{d,k}) = E_{v(\widetilde{\Delta\tau})}\left[\frac{6}{(2\pi)^2\frac{A^2|v(\widetilde{\Delta\tau})|^2}{\sigma^2}f_s T_{coh}^3}\right]. \quad (18)$$

This expectation in (18) is far from trivial to calculate. For this reason, we compute an extensive number of Monte Carlo iterations and then, we calculate the mean of all iterations to obtain the value of $\mathrm{ECRB}(f_{d,k})$.

IV. Simulation Results

Simulations are carried out by the use of $\mathrm{BOC}_{\cos}(15,2.5)$ signals, as a particular case of high-order BOC modulations, using a coherent time of 10 ms, and a sampling frequency of 50 MHz. We consider a frequency search range from - 500 Hz to 500 Hz since we assume knowing the assisted information about the Doppler frequency from the satellite and the steps of the search frequency are every 50 Hz. Moreover, simulations are performed in an AWGN channel and including an unknown random code-delay at the received signal, which follows a uniform distribution.

To measure the performance of the LS and MLS estimators, the mean square error (MSE) is used

$$f_{\mathrm{MSE}} = E\left[\left(f_{d,k} - \hat{f}_{d,k}\right)^2\right], \quad (19)$$

which is computed by averaging 3000 Monte Carlo iterations for each value of $\mathrm{C/N_0}$.

Fig. 4 shows the MSE of the LS estimator, MLS estimator, CRB, and ECRB. In this case, we use $C = 3$ for the MLS estimator. The rationale for that will be explained later on. The result shows that the MLS estimator is the best estimator because it provides an improvement over the LS estimator in terms of accuracy in Doppler frequency estimation. The MLS estimator allows us to recover a part of the energy lost in the CAF by the unknown random difference between the code-delay of the received signal and the local replica. Therefore, the usage of several peaks from the CAF lead to a frequency estimation more accurate than only using the main peak from the CAF. However, the MLS estimator is not able to reach the CRB value. It should be added that the LS estimator has also a good performance because it is very close to the ECRB.

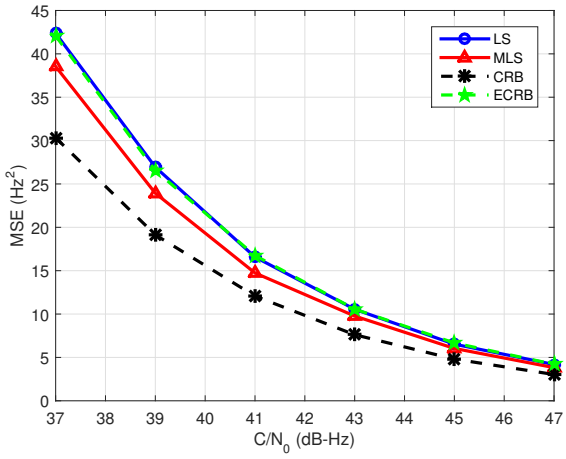

Fig. 4. MSE of the MLS and LS estimators using a $f_s = 50$ MHz.

It should also be noted that, in the Fig. 4, the CRB indicates the best estimate of the Doppler frequency that one estimator can get because it depends on the $\mathrm{C/N_0}$ of the received signal. For this reason, the LS and MLS estimators cannot improve the performance of this bound. The ECRB has been calculated assuming that the $\mathrm{C/N_0}$ of the received signal is the maximum value of the peak of the CAF, which is affected by the unknown code-delay between the received signal and the local replica. However, the $\mathrm{C/N_0}$ value used to calculate the ECRB is not completely true because the real value of $\mathrm{C/N_0}$ is the one obtained from the received signal. As a result, the bound that we cannot improve is the CRB, but there may be estimators between the ECRB and the CRB.

In order to find the optimum number of chosen large values of the CAF in time domain C, we carry out an extensive number of simulations with different values of C. Fig. 5 shows the division between the MSE using the MLS estimator with $C = 3$, $C = 5$, and $C = 10$ and the MSE of the LS estimator. The result shows that it makes little difference when the value of C is changed for values such as 3 or 5. Nevertheless, MLS has always the best performance for $C = 3$ using a $f_s = 50$ MHz. The larger the number of C, the more degradation the MLS suffers. Moreover, although we do not use the optimal value of C, the MLS estimator might provide an improvement over the LS estimator.

Fig. 6 shows the comparison between the LS estimator and the ECRB for different values of f_s. In this simulation, we analyze the effect of the sampling frequency used in the receiver, which affects to the separation among the samples of the CAF in the acquisition stage. This fact causes that the precision in the Doppler frequency estimation must be different since it depends on the value of $E[v(\widetilde{\Delta\tau})]$.

We choose several values of f_s, such as 40 MHz, 62 MHz and 100 MHz, to perform the simulation. In this case, the results show that the most accurate estimation of the Doppler frequency is provided using 100 MHz. Intuitively, one can think the larger the f_s, the more accurate the estimation of the

978-1-5090-3885-5/16/$31.00 ©2016 IEEE

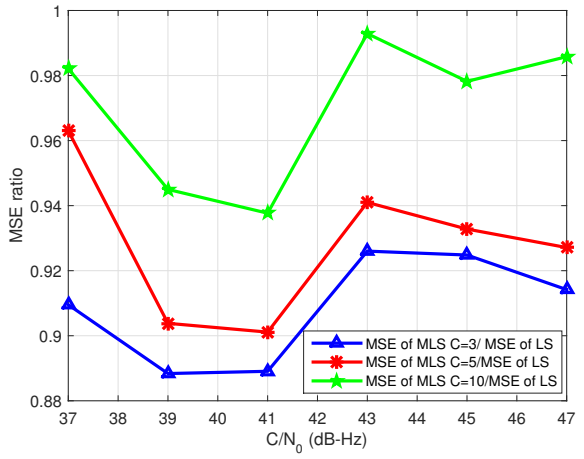

Fig. 5. The division between the MSE applying the MLS estimator with $C=3$, $C=5$, and $C=10$ and the MSE of the LS estimator using a $f_s=50$ MHz.

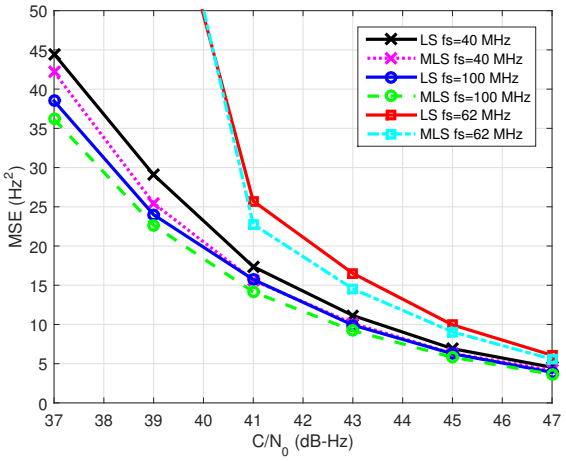

Fig. 7. Comparison between the MLS and LS estimators using $f_s=40$, 62 and 100 MHz.

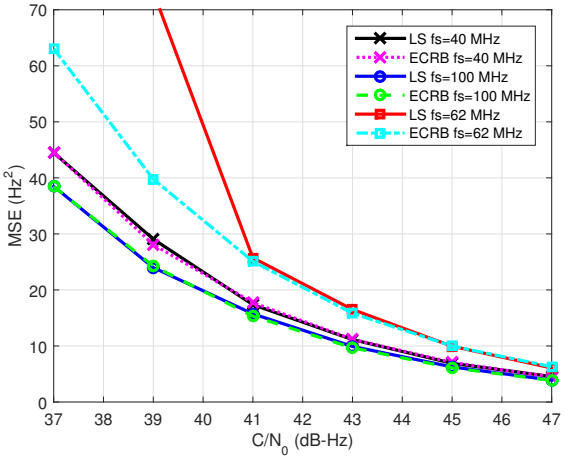

Fig. 6. MSE comparison using $f_s=40$, 62 and 100 MHz.

Doppler frequency because the separation among the samples in the CAF is smaller. Nevertheless, it does not always follow this rule, as it can be seen for the case of $f_s=40$ MHz and $f_s=62$ MHz. This happens because the separation among the samples of the received signal using a $f_s=62$ MHz is really similar to the distance between the peaks in the CAF of the $\text{BOC}_{\cos}(15,2.5)$ signal. More precisely, the distance between the peaks of a BOC correlation is given by $1/(2f_{sub})$, where f_{sub} is sub-carrier frequency. In particular, the f_{sub} of a $\text{BOC}_{\cos}(15,2.5)$ signal is $15\cdot 1.023$ MHz. In this situation, using a $f_s=62$ MHz, we have approximately two samples equidistant for each peak of the correlation. The CAF of the $\text{BOC}_{\cos}(15,2.5)$ signal is sampled in all the different peaks of the correlation function of the same way, but any secondary peak cannot outperform the magnitude of the main peak (without presence of noise). However, using the $f_s=40$ MHz, this effect does not happen because the separation among the samples of the received is not equidistant compare to the distance between the peaks of the $\text{BOC}_{\cos}(15,2.5)$ correlation and, in this case, the magnitude of a secondary peak can outperform the value of the main peak.

This fact causes the value of $E[\nu(\widetilde{\Delta\tau})]$ for $f_s=40$ MHz is larger than the value of $E[\nu(\widetilde{\Delta\tau})]$ for $f_s=62$ MHz. For this reason, the estimation of the Doppler frequency can be more accurate using $f_s=40$ MHz than $f_s=62$ MHz. Moreover, it also produces that the MSE of the LS using $f_s=62$ MHz needs a larger C/N_0 to reach its ECRB since we have a larger number of false alarm using this value of f_s. In addition to this, we also prove the MLS estimator for values of $f_s=40$, 62, and 100 MHz in Fig. 7. In all the cases, the MLS estimator improves the performance of the LS estimator.

V. Conclusions

In this work, a new technique is proposed, which is so-called multilag least squares estimator, to refine the Doppler frequency estimation obtained in the acquisition stage. This technique exploits the secondary peaks provided by the CAF of a high-order BOC signal to get an accurate estimation of the Doppler frequency. The MLS estimator outperforms the LS estimator proposed in the literature. The optimum number of chosen large values of the CAF is 3 to obtain the most accurate estimation of Doppler frequency using a sampling frequency of 50 MHz. Moreover, the advantage of the MLS estimator is that it can be applied in any receiver since it only uses the CAF generated in the acquisition stage. In addition, we have analyzed the dependence between the sampling frequency used to acquire the signal and the accuracy to estimate the Doppler frequency.

References

[1] G. Seco-Granados, J. Lopez-Salcedo, D. Jimenez-Banos, and G. Lopez-Risueno, "Challenges in indoor global navigation satellite systems: Unveiling its core features in signal processing," *IEEE Signal Processing Magazine*, vol. 29, no. 2, pp. 108–131, March 2012.

978-1-5090-3885-5/16/$31.00 ©2016 IEEE

[2] J. T. Curran, G. Lachapelle, and C. C. Murphy, "Improving the design of frequency lock loops for GNSS receivers," *IEEE Transactions on Aerospace and Electronic Systems*, vol. 48, no. 1, pp. 850–868, Jan 2012.
[3] E. Kaplan and C. Hegarty, *Understanding GPS: principles and applications*. Artech house, 2005.
[4] X. Tang, E. Falletti, and L. Lo Presti, "Fast nearly ML estimation of Doppler frequency in GNSS signal acquisition process," *Sensors*, vol. 13, no. 5, pp. 5649–5670, 2013.
[5] C. Ma, G. Lachapelle, and M. E. Cannon, "Implementation of a software GPS receiver," in *ION GNSS*, 2004, pp. 21–24.
[6] X. Tang, E. Falletti, and L. L. Presti, "Fine Doppler frequency estimation in GNSS signal acquisition process," in *6th ESA Workshop on Satellite Navigation Technologies and European Workshop on GNSS Signals and Signal Processing, (NAVITEC)*, Dec 2012, pp. 1–6.
[7] E. Commission, "European GNSS (Galileo) Open Service. Signal in Space Interface Control Document," 2011.
[8] J. A. Garcia-Molina, M. Navarro-Gallardo, G. Lopez-Risueño, and M. Crisci, "Unambiguous tracking of high-order BOC signals in urban environments: Channel considerations," in *IEEE 7th ESA Workshop on Satellite Navigation Technologies and European Workshop on GNSS Signals and Signal Processing (NAVITEC)*, 2014, pp. 1–6.
[9] M. Navarro-Gallardo, G. Lopez-Risueo, M. Crisci, and G. Seco-Granados, "Analysis of side lobes cancellation methods for BOCcos(n, m) signals," in *6th ESA Workshop on Satellite Navigation Technologies and European Workshop on GNSS Signals and Signal Processing, (NAVITEC)*, Dec 2012, pp. 1–7.
[10] D. Borio, "Double phase estimator: new unambiguous binary offset carrier tracking algorithm," *IET Radar, Sonar Navigation*, vol. 8, no. 7, pp. 729–741, Aug 2014.
[11] E. S. Lohan, A. Burian, and M. Renfors, "Low-complexity unambiguous acquisition methods for BOC-modulated CDMA signals," *International Journal of Satellite Communications and Networking*, vol. 26, no. 6, pp. 503–522, 2008. [Online]. Available: http://dx.doi.org/10.1002/sat.922
[12] J. A. Garcia-Molina, M. Navarro-Gallardo, G. Lopez-Risueño, and M. Crisci, "Robust unambiguous tracking of high-order BOC Signals: a multi-Correlator approach," in *ION GNSS*, September 2015.
[13] D. Gómez-Casco, J. A. López-Salcedo, and G. Seco-Granados, "Generalized Integration Techniques for High-Sensitivity GNSS Receivers Affected by Oscillator Phase Noise," in *IEEE Statistical Signal Processing Workshop (SSP)*, 2016.
[14] L. L. Presti, X. Zhu, M. Fantino, and P. Mulassano, "GNSS signal acquisition in the presence of sign transition," *IEEE Journal of Selected Topics in Signal Processing*, vol. 3, no. 4, pp. 557–570, Aug 2009.
[15] S. M. Kay, "Fundamentals of statistical signal processing, volume i: estimation theory," 1993.
[16] E. Reserch, "USRP N200/N210 NetwQrked Series," *Moun- tain Viewi CA: Ettus Research*, 2012.
[17] S. Reisenfeld and E. Aboutanios, "A new algorithm for the estimation of the frequency of a complex exponential in additive Gaussian noise," *IEEE Communications Letters*, vol. 7, no. 11, pp. 549–551, Nov 2003.
[18] H. L. Van Trees and K. L. Bell, "Bayesian bounds for parameter estimation and nonlinear filtering/tracking," *AMC*, vol. 10, p. 12, 2007.

978-1-5090-3885-5/16/$31.00 ©2016 IEEE